Computational and Experimental Investigation of the Transformation of V_2O_5 Under Pressure

J. M. Gallardo-Amores,[†,‡] N. Biskup,[§] U. Amador,[∥] K. Persson,[⊥] G. Ceder,[⊥] E. Morán,[†,‡] and M. E. Arroyo y de Dompablo*[,†]

Departamento de Química Inorgánica, Universidad Complutense de Madrid, 28040 Madrid, Spain, Laboratorio de Altas Presiones, Universidad Complutense de Madrid, 28040 Madrid, Spain, Instituto de Ciencia de Materiales de Madrid, CSIC, 28049 Cantoblanco, Madrid, Spain, Departamento de Química, Universidad San Pablo-CEU, 28668 Boadilla del Monte, Spain, and Department of Materials Science and Engineering, Massachusetts Institute of Technology, 77 Massachusetts Avenue, Cambridge, Massachusetts 02139-4307

Received May 19, 2007. Revised Manuscript Received July 28, 2007

It has previously been reported that under high-pressure V_2O_5 (α-V_2O_5) transforms into a layered polymorph, β-V_2O_5, consisting of $V^{5+}O_6$ octahedra instead of $V^{5+}O_5$-square pyramids. Both polymorphs have a good performance as positive electrode for lithium batteries. In this work, we investigate the pressure-induced $\alpha \rightarrow \beta$ transformation combining first principles and experimental methods. Density functional theory (DFT) predicts that α-V_2O_5 transforms to β-V_2O_5 at 3.3 GPa with a 11% volume contraction; experiments corroborate that at a pressure of 4 GPa, V_2O_5 ($d = 3.36$ g/cm^3) transformed into a well-crystallized β-V_2O_5, with a much denser structure ($d = 3.76$ g/cm^3). β-V_2O_5 can be also prepared at 3 GPa, although with a substantial degree of amorphization. The calculated bulk modulus of α-V_2O_5 (18 GPa) indicates that this is a very compressible structure; this being linked to the contraction along its *b*-axis (interlayer space) and to a significant decrease of a long V−O distance (V−O ≈ 2.9 Å). As a result, the vanadium coordination increases from five (square pyrmamid) in α-V_2O_5 to six (distorted octahedron), leading to the stabilization of the high-pressure (β) polymorph. This change of the coordination environment of vanadium ions also affects the electrical conductivity. The calculated density of states shows a narrowing of 0.5 V in the band gap for the β polymorph, in comparison to the ambient-pressure material; the measured resistivities at room temperature (10 000 Ω cm in α-polymorph and 400 Ω cm in β-polymorph) reveal that β-V_2O_5 is indeed a better electronic conductor than α-V_2O_5. In view of these results, similar transformations at moderate pressures are expected to occur in other V^{5+} frameworks, suggesting an interesting way to synthesize novel V^{5+} compounds with potential for electrochemical devices.

Introduction

Pentavalent-vanadium-based frameworks constitute an important class of materials because of their applications for energy storage.[1−12] The high redox potential of the V^{5+}/V^{4+} couple versus lithium (3.5 V) ensures that a high energy can be delivered by V^{5+} materials when used as positive electrode in lithium cells. In most cases, V^{5+} compounds crystallize in open structures, enabling a fast and reversible lithium intercalation reaction. In particular, V_2O_5 ranks among the most studied materials as a positive electrode for lithium cells because of its high-energy density and capacity retention upon cycling.[13−15] In this regard, it is interesting to explore possible structural transformations of V_2O_5 that could lead to novel polymorphs with potential for electrochemical applications. High-pressure/high-temperature routes (HP/HT) are widely used to induce structural transformations of materials, leading to novel polymorphs possessing structures

* To whom correspondence should be addressed. Phone: +34 91 3945168. Fax: +34 914352. E-mail address: e.arroyo@quim.ucm.es.
[†] Departmento de Química Inorgánica, Universidad Complutense de Madrid.
[‡] Laboratorio de Altas Presiones, Universidad Complutense de Madrid.
[§] Instituto de Ciencia de Materiales de Madrid.
[∥] Departamento de Química, Universidad San Pablo-CEU.
[⊥] Department of Materials Science and Engineering, Massachusetts Institute of Technology.

(1) Saidi, M. Y.; Koksbang, R.; Saidi, E. S.; Barker, J. *Electrochim. Acta* **1997**, *42* (8), 1181−1187.
(2) Rozier, P.; Savarialut, J.-M.; Galy, J. *J. Solid State Chem.* **1996**, *122*, 303.
(3) Rozier, P.; Savarialut, J.-M.; Galy, J. *Solid State Ionics* **1997**, *98*, 133.
(4) Prakash, A. S.; Rozier, P.; Dupont, L.; Vezin, H.; Sauvage, F.; Tarascon, J. M. *Chem. Mater.* **2006**, *18* (2), 407−412.
(5) Potiron, E.; Le Gal La Salle, A.; Verbaere, A.; Piffard, Y.; Guyomard, D.; Tournoux, M. *J. Phys. Chem. Solids* **2001**, *62*, 1447.
(6) Potiron, E.; Lasalle, A. L.; Verbaere, A.; Piffard, Y.; Guyomard, D. *Electrochim. Acta* **1999**, *45* (1−2), 197−214.
(7) Julien, C. M. *Mater. Sci. Eng. R* **2003**, *40* (2), 47−102.
(8) Morcrette, M.; Rozier, P.; Dupont, L.; Mugnier, E.; Sannier, L.; Galy, J.; Tarascon, J.-M. *Nat. Mater.* **2003**, *2*, 755.
(9) Chirayil, T.; Zavalij, P. Y.; Whittingham, M. S. *J. Mater. Chem.* **1997**, *7*, 2193.
(10) Benedek, R.; Thackeray, M. M.; Yang, L. H. *Phys. Rev. B: Condens. Matter* **1997**, *56* (17), 10707−10710.
(11) Delmas, C.; Brèthes, S.; Ménétrier, M. *J. Power Sources* **1991**, *34*, 113.
(12) Zavalij, P.; Whittingham, M. S. *Acta Crystallogr.* **1999**, *B55*, 627−663.
(13) Delmas, C.; Cognac-Auradou, H. Cocciantelli, J. M.; Ménétrier, M.; Doumerc, J. P. *Solid State Ionics* **1994**, *69*, 257−264.
(14) Murphy, D. W.; Christian, P. A.; Disalvo, F. J.; Waszczak, J. V. *Inorg. Chem.* **1979**, *18*, 2800.
(15) Dickens, P. G.; French, S. J.; A. T., H.; Pye, M. F. *Mater. Res. Bull.* **1979**, *14*, 1295.

10.1021/cm071360p CCC: $37.00
Published on Web 09/27/2007

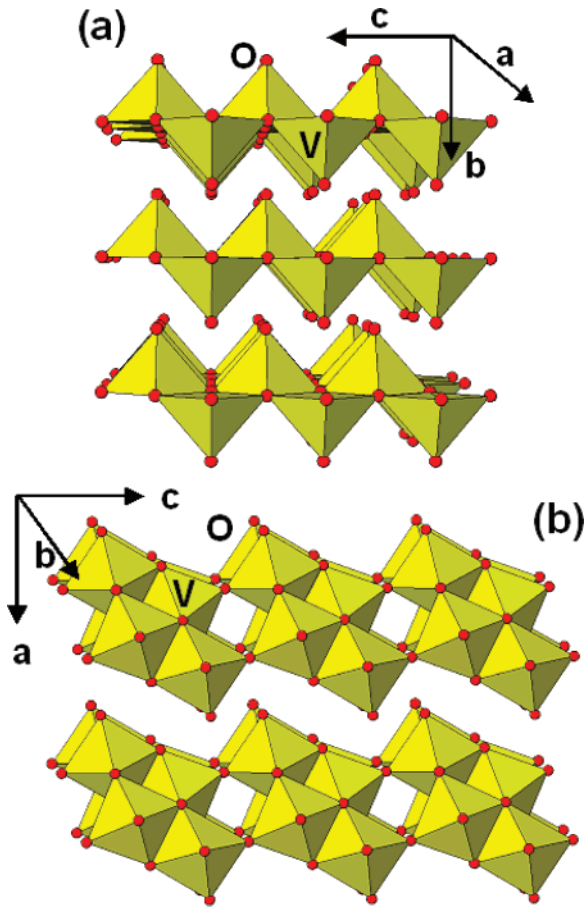

Figure 1. Schematic structures of (a) α-V_2O_5 and (b) β-V_2O_5. The settings for the unit cell axes are those used in the ab initio calculations.

not accessible at ambient pressure. Thus, high-pressure forms of V_2O_5 and other V^{5+}-based compounds could constitute a new class of materials for electrochemical applications.

At ambient pressure (AP), V_2O_5 (the α-polymorph according to Balog et al.)[16] crystallizes in a layered structure consisting of VO_5-square pyramids sharing their vertices and corners (Figure 1a). It has been recently reported that V_2O_5 transforms at 6 GPa to a monoclinic polymorph (hereafter, β-V_2O_5), where the V atoms are six-coordinated by oxygen in distorted VO_6 octahedra.[17] The structure is built up from quadruple units of edge-sharing VO_6 octahedra linked by sharing edges along [100] and mutually connected by sharing corners along [001] (see Figure 1b). This arrangement forms layers with composition V_4O_{10} in planes parallel to (100). The layers are held together by weak forces, suggesting that this compound could host lithium ions as does the ambient-pressure polymorph. In fact, we have recently reported that lithium ions can be reversibly intercalated in this high-pressure polymorph,[18] leading to the formation of a lithium vanadium bronze of the composition $Li_xV_2O_5$ ($x \leq 2$) with the Li atoms located between the V_4O_{10} double layers. The framework of the high-pressure (β) polymorph is stable at ambient pressure and is retained during the cycling of the β-V_2O_5||Li cells, delivering a specific capacity of 250 Ah/Kg at a *C*/3.5 rate, this is to say, comparable to that of the ambient pressure polymorph. With these electrode characteristics, one can say that the layered structure of β-V_2O_5 allows a good lithium mobility, despite being a denser structure than the AP polymorph.

Pressure induces a change in the coordination environment around the vanadium ions from square pyramidal in α-V_2O_5 to octahedral in β-V_2O_5; such a transformation could occur in other frameworks based on square-pyramids V^{5+}. The potential electrochemical application of (AP/HP)-V_2O_5 opens new perspectives to other V^{5+}-host materials that could exhibit a similar transformation under pressure. To investigate this possibility, in this work, we seek a better understanding of the physical and chemical aspects involved in the V_2O_5 polymorphic transformation. In this connection, in a recent paper, Balog et al.[16] revisited the P−T phase diagram of V_2O_5, but these authors did not analyze either the structural details related to the α → β transition or the changes in the electronic structure.

The pressure required to induce the transformation is a key point because, in terms of applications, the disadvantages of HP electrode materials are their high-cost and energy-consuming synthesis. A moderate transformation-pressure makes feasible large-scale production and lower cost. Determination of the minimum pressure required to induce a phase transformation could demand numerous experiments on a *trial-and-error* basis. However, transformation of materials under pressure can be well studied from the first principles methods even under extreme conditions, such as pressures relevant to the interior of the Earth. At $T = 0$ K, the transition pressure, P_t, corresponds to the point where the two involved structures have the same enthalpy. A good estimate of the transition pressure, P_t, can be obtained from the calculated total energy as a function of the volume for each phase, being the slope of the tangent line between the two E(V) curves. In the first part of this work, we have performed a first principles investigation to evaluate the minimum pressure required to induce the α → β transformation in V_2O_5. Experimental work has been done, guided by the predictions. The evolution of lattice parameters and bond lengths with pressure has also been investigated from first principles.

Generally speaking, HP materials are better electronic conductors than their corresponding AP polymorphs. The enhanced electronic conductivity of HP-polymorphs can reduce the polarization of the lithium cell and improve the power capability. In the second part of this work, we have combined experimental and first principles methods to investigate the electronic structure and electrical conductivity of AP and HP (β) V_2O_5 polymorphs. Information on the *intrinsic* electronic conductivity can be inferred from the calculated density of states. The electronic structure of the AP and β polymorphs is expected to vary depending on the relevant structural aspects that accompany the transformation, namely, the variation in the vanadium environment from a square-pyramid coordination in α-V_2O_5 to an octahedral coordination in β-V_2O_5.

(16) Balog, P.; Orosel, D.; Cancarevic, Z.; Schön, C.; Jansen, M. *J. Alloys Compds.* **2007**, *429*, 87−98.
(17) Filonenko, V. P.; Sundberg, M.; Werner, P. E.; Zibrov, I. P. *Acta Crystallogr.* **2004**, *B 60*, 375.
(18) Arroyo y de Dompablo, M. E.; Gallardo-Amores, J. M.; Amador, U.; Moran, E. *Electrochem. Commun.* **2007**, *9* (6), 1305−1310.

Methodology

Computational. We have performed total energy calculations based on the density functional theory (DFT) within the generalized gradient approximation (GGA) as implemented in the VASP[19−21] package. For the exchange and correlation functional, we chose a form suggested by Perdew, Burke, and Ernzerhof (PBE).[22] A number of six- and eleven-valence electrons were considered for O ($1s^2\ 2s^1\ 3p^6$) and V ($3p^6 4s^2 d^3$), respectively, while the remaining core electrons, together with the nuclei, are described by pseudopotentials following the projector augmented wave (PAW) formalism.[23] The wave functions were expanded with a plane-wave basis set with a cutoff kinetic energy of 500 eV. The integration in the Brillouin zone is done by using the tetrahedron method as corrected by Blöchl on a set of *k*-points ($4 \times 6 \times 6$ and $4 \times 6 \times 4$ for α-V_2O_5 and β-V_2O_5, respectively) determined by the Monkhorst−Pack scheme (36 and 24 irreducible *k*-points for β-V_2O_5 and β-V_2O_5, respectively). Using these parameters, a total-energy convergence close to 5 meV per formula unit was achieved. The initial cell parameters and atomic positions of α-V_2O_5 and β-V_2O_5 were taken from refs 24 and 17, respectively, with the unit cell containing two formula units (V_2O_{10}). As a first step the structures were fully relaxed (cell parameters and atomic positions); the final energies of the optimized geometries were recalculated so as to correct for the changes in the basis set of the wave functions during relaxation. Second, relaxed structure calculations were performed at various constant volumes and the energy-volume data was fitted to the Murnaghan equation of state[25]

$$E(V) = B_0 V_0 \left[\frac{1}{B'(B'-1)} \left(\frac{V_0}{V} \right)^{B'-1} + \frac{V}{B'V_0} - \frac{1}{(B'-1)} \right] + E_0 \qquad (1)$$

where B_0 is the bulk modulus at zero pressure, B' its first derivative, E_0 the minimum energy, and V_0 the volume at the minimum of energy. Preparation and analysis of VASP files were done primarily with the CONVASP code.[26]

Experimental Section

Commercial (α-polymorph) (Aldrich) V_2O_5 was subjected at 3, 4, 6, and 8 GPa and 800 °C for 1 h in a belt-type press. For comparison purposes, the material was also prepared in a Conac press at 4 GPa. The latter allows a more homogeneous hydrostatic pressure because its spherical geometry. The resulting samples were examined by X-ray diffraction performed on a Bruker D8 high-resolution X-ray powder diffractometer, using monochromatic Cu $K\alpha_1$ ($\lambda = 1.5406$ Å) radiation obtained with a germanium primary monochromator and equipped with a position-sensitive detector (PSD) MBraun PSD-50M. The treatment of the diffraction data was carried out using the FullProf program.[27] Samples were also examined by scanning electron microscopy (SEM) on a JEOL 6400 microscope equipped with an EDAX Inc., energy-dispersive X-ray detector for microanalysis.

(19) Kresse, G.; Furthmuller, J. *Comput. Matter Sci.* **1996**, *15*, 6.
(20) Liechtenstein, A. I.; Anisimov, V. I.; Zaanen, J. *Phys. Rev. B* **1995**, *52* (8), R5467−R5470.
(21) Kresse, G.; Furthmuller, J. *Phys. Rev. B* **1996**, *54*, 169.
(22) Perdew, J. P.; Burke, K.; Ernzerhof, M. *Phys. Rev. Lett.* **1996**, *77* (18), 3865−3868.
(23) Bloch, P. E. *Phys. Rev. B* **1994**, *50*, 17953.
(24) Enjalbert, R.; Galy, J. *Acta Crystallogr.* **1986**, *C42*, 1467.
(25) Murnaghan, F. D. *Proc. Natl. Acad. Sci. U.S.A.* **1944**, *30*, 244.
(26) Morgan, D.; Curtarolo, S.; Ceder, G. http://burgaz.mit.edu/PUBLICATIONS/codes.php.
(27) Rodriguez-Carvajal, J. *Fullprof*; Satellite Meeting on Powder Diffraction of the XV Congress of the IUCr, Toulouse, France, 1990; PUBLISHER: Toulouse, France, 1990.

Table 1. Ground State Structural Parameters for α-V_2O_5 and β-V_2O_5 Calculated within the DFT in Comparison with Experimental Values[17,24]

compound	experimental	calculated	error (%)
α-V_2O_5	$a = 11.512$ Å	$a = 11.627$ Å	0.9
	$b = 4.371$ Å	$b = 4.538$ Å	3.6
	$c = 3.564$ Å	$c = 3.577$ Å	0.4
	$V = 179.33$ Å^3	$V = 188.76$ Å^3	4.9
	$d = 3.36$ gcm^{-3}	$d = 3.20$ gcm^{-3}	
β-V_2O_5	$a = 7.1225(4)$ Å	$a = 7.440$ Å	4.2
	$b = 3.5769(3)$ Å	$b = 3.571$ Å	0.1
	$c = 6.2967(2)$ Å	$c = 6.368$ Å	1.1
	$\beta = 90.23(4)°$	$\beta = 89.97°$	
	$V = 160.41(2)$ Å^3	$V = 169.21$ Å^3	5.2
	$d = 3.76$ gcm^{-3}	$d = 3.57$ gcm^{-3}	
cell contraction	11.8%	11.6%	

Once β-V_2O_5 was obtained, its phase transition back to the ambient pressure polymorph was analyzed by differential scanning calorimetry using a Perkin−Elmer Pyris 1 system between 50 and 450 °C. The heating rate was 10 °C/min to 450 °C, and oxygen was used as purge gas.

For transport measurements, commercial α-V_2O_5 powder was conformed into 13 mm diameter pellets by uniaxially applying a pressure of 0.37 kbar and sintering for 12 h at 650 °C. Pelletized β-V_2O_5 was used as obtained from the HP-press. DC transport measurements in the temperature region of $77 < T < 300$ K have been done in both 4-contact and 2-contact configurations. A Keithley sourcemeter or a combination of a standard current source and a voltmeter was used for 2-contact and 4-contact measurements, respectively.

Results and Discussion

Transition Pressure and Mechanism of the Transformation. *Computational.* We determined, from DFT, the lowest pressure needed to induce the transformation of α-V_2O_5 into the β polymorph. Table 1 compares the calculated lattice parameters for the fully relaxed structures of the α- and β-V_2O_5 polymorphs with the experimentally reported values. The calculated parameters are overestimated, as usually found within the GGA approximation. The calculated axis length along the interlayer space (*b* in α-V_2O_5 and *a* in β-V_2O_5) presents the maximum deviation from the experimental results, about 5%. It is worth mentioning that the calculated volume contraction between the α- and the β-polymorph is 11.8%, which agrees very well with the experimental value of 11.6%. The calculated density of β-V_2O_5 is 3.6 g/cm^3, to be compared with 3.2 g /cm^3 of the ambient pressure V_2O_5.

Table 2 summarizes the calculated and experimental V−O distances in both the α- and β-V_2O_5 polymorphs. In α-V_2O_5, the vanadium ions are located in square pyramid environments, which can be considered as a distorted octahedron with a short V−O bond at 1.58 Å (vanadyl bond) and a long V−O distance of 2.79 Å; the latter interatomic contact, which defines the length between layers, is too long to be considered a real bond. In the β-V_2O_5 polymorph, the vanadium ions are 6-fold coordinated in two types of highly distorted VO_6 octahedra; the vanadium ions are off-center, yielding short bond distances of 1.65 and 1.58 Å, the latter being typical of a vanadyl group. Opposite to these short bonds are oxygen atoms at 2.30 Å, which can be considered bonded to the vanadium ions. The local vanadium ion environments in the

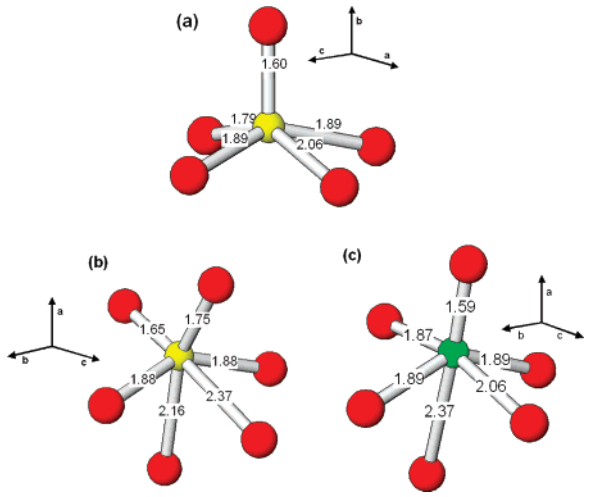

Figure 2. Coordination polyhedron of vanadium ions in (a) α-V_2O_5 and (b, c) in β-V_2O_5 where vanadium ions are located in two different distorted octahedral environments.

Table 2. Experimental[17,24] and Calculated V−O Interatomic Distances (Å) for the V_2O_5 Polymorphs

			calculated V−O distances (Å)			
compound	experimental V−O distances (Å)			error (%)		error (%)
α-V_2O_5	1.577(3)		1.601	1.54		
	1.779(2)		1.792	0.74		
	1.878(1)		1.891	0.68		
	1.878(1)		1.891	0.68		
	2.017(3)		2.055	1.89		
	2.791(3)		2.938	5.24		
β-V_2O_5	1.649(6)	1.583(6)	1.654	0.27	1.592	0.55
	1.704(7)	1.871(2)	1.751	2.75	1.878	0.39
	1.872(2)	1.871(2)	1.876	0.20	1.89	1.03
	1.872(2)	1.882(8)	1.876	0.20	1.89	0.44
	2.176(6)	2.060(8)	2.172	0.18	2.066	0.29
	2.308(6)	2.295(6)	2.376	2.92	2.373	3.40

optimized structures of α- and β-V_2O_5 are represented in Figure 2. Broadly speaking, there is a good agreement between calculated and experimental data, though the long V−O distance in α-V_2O_5 is overestimated (exptl 2.79 Å vs calcd 2.93 Å) according to the aforementioned overprediction of the *b*-axis.

Starting from the optimized structures, we performed several fixed-volume calculations. Computationally, one can preserve the α-V_2O_5 phase at pressures far above the transition point, provided that the symmetry constraints of the *Pmnm* space group are imposed. Figure 3a shows the calculated total energy as a function of the volume per atom for α-V_2O_5 (diamonds) and β-V_2O_5 (squares), together with the corresponding fit of the DFT data to the Murnagham equation of state (1).[25] As expected, the global energy minimum corresponds to α-V_2O_5, the polymorph stable at ambient pressure. The curves of the α- and β-polymorphs cross at a volume of approximately 12 $Å^3$ per atom, indicating that β-V_2O_5 becomes more favorable at sufficiently high pressure. Figure 3b shows the calculated enthalpy-pressure variation for both the α- and β-polymorphs. It can be observed that β-V_2O_5 is effectively predicted as the thermodynamically stable phase above 3.3 GPa; this is well below the 6 GPa used by Filonenko et al.[17] and Kusaba et al.[28] in their quenching experiments. A pressure on the order of 3 GPa means that β-V_2O_5 could be prepared in a piston-cylinder type-press or maybe even achieved by high-energy ball-milling, thus potentially decreasing the cost of the high-pressure synthetic process.

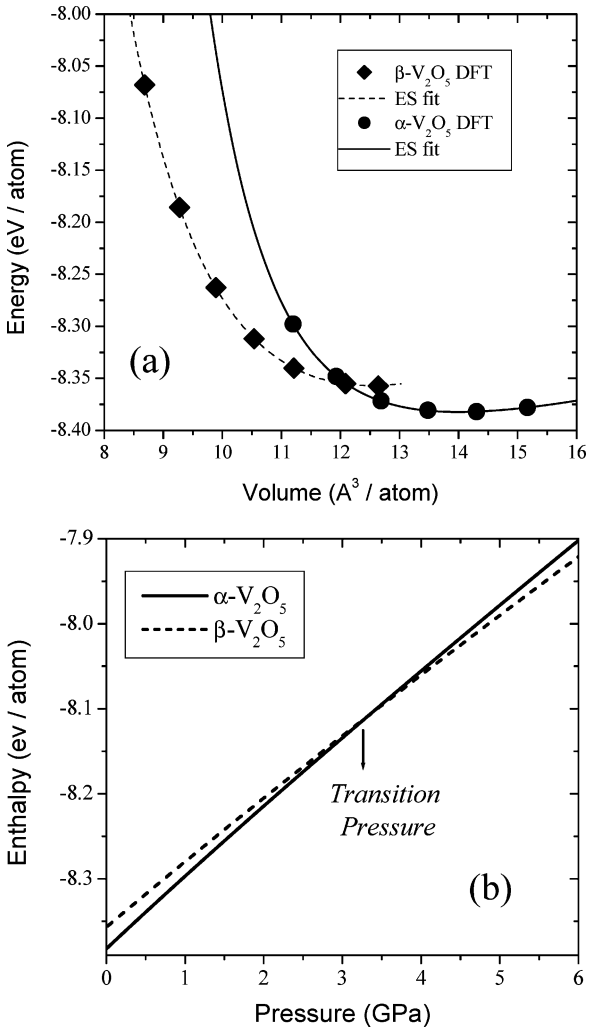

Figure 3. (a) Total energy vs volume curves for α-V_2O_5 and β-V_2O_5. Symbols correspond to the DFT calculated data, and lines show the fitting to the Murnagham equation of state. (b) Enthalpy per atom vs pressure for α-V_2O_5 (continuos line) and β-V_2O_5 (dashed line).

Table 3. Calculated Equation of State Parameters for V_2O_5 Polymorphs[a]

compound	B_0 (GPa)	B_0'	V_0 ($Å^3$)	E_0 (eV)	rms (meV)
α-V_2O_5	18.828	9.961	13.99	−8.382	0.07
β-V_2O_5	29.867	5.986	12.53	−8.357	0.18

[a] All the Results are Given Per Atom. E_0, V_0, B_0 and B_0' are the Zero-pressure Energy, Volume, Bulk Modulus and Its Pressure Derivative, Respectively.

Table 3 reports the parameters of the Murnaghan equation of state fitted to the ab initio $E(V)$ data. The α-V_2O_5 phase exhibits a bulk modulus of 18 GPa, signifying that it is very compressible. Figure 4a displays the calculated changes in the lattice parameters as a function of pressure for this AP-polymorph (DFT data). The dashed line corresponds to the

(28) Kusaba, K.; Ohshima, E.; Syono, Y.; Kikegawa, T. *J. Cryst. Growth* **2001**, *229*, 467−471.

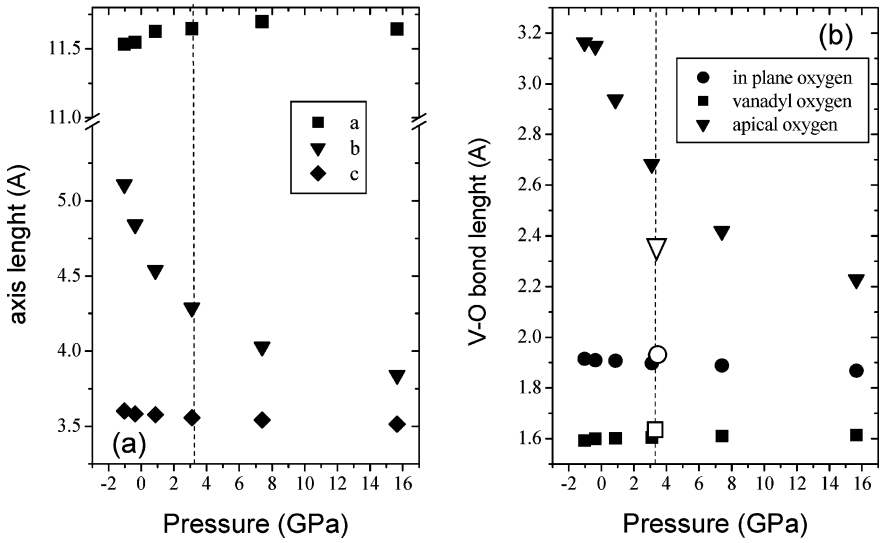

Figure 4. Calculated pressure dependence of the (a) lattice parameters and (b) V−O bond lengths for α-V_2O_5 (space group *Pmnm*). The dashed line indicates the pressure of the transformation to the β-V_2O_5 (3.3 GPa). The white symbols correspond to the V−O distances in the β-V_2O_5.

transition pressure at which the β-V_2O_5 structure becomes thermodynamically more favorable. The compressive behavior is highly anisotropic; the *b*-axis decreases remarkably, whereas the *a* and *c* axes barely change. This behavior is also conveyed in the evolution of the V−O bond lengths, shown in Figure 4b. While the in-plane V−O distance and the vanadyl bond vary slightly under pressure, the axial long-V−O distance reduces by 0.9 Å in the pressure range studied. This indicates that the polymorphic transformation is caused by the stabilization under pressure of octahedrally coordinated vanadium ions, in contrast to the square pyramidal environment of vanadium ions that characterizes the ambient-pressure V_2O_5 polymorph (see Table 2 and Figure 2). Thus, similar transformations can be expected to occur in other compounds based on V^{5+} ions in square-pyramid coordination opening up promising perspectives to prepare novel V^{5+}-intercalation compounds.

The DFT data revealed the importance of the pronounced reduction of the interlayer space in α-V_2O_5 occurring along the pressure-induced phase transition. Noteworthy, despite the significant pressure-induced contraction along the *b*-axis in α-V_2O_5, the β-V_2O_5 polymorph is still a layered structure, although with a narrower interlayer distance (see Figure 1). The calculated bulk modulus of β-V_2O_5 (30 GPa) also suggests that this form is rather compressible. Hence, another polymorph of V_2O_5 could exist at higher pressures, in which the interlayer space would collapse to give a 3D framework. Such a possibility has been previously pointed out by several authors,[17,29,30] and recently, the structure of the new polymorph δ-V_2O_5, prepared at 9.5 GPa, has been reported.[16] This polymorph presents a rutile-related structure with a 3D character.

Experimental. α-V_2O_5 treated at 3−8 GPa and 800 °C turns into a black-reddish powder, and independently of the pressure used in the experiments, the patterns of all the samples can be indexed with the unit cell previously proposed for β-V_2O_5.[17] Figure 5a shows the XRD pattern of the sample obtained at 4 GPa, which was used for all the physical measurements. The final cell parameters are a = 7.1216(3) Å, b = 3.5720 (3) Å, c = 6.2882 (2)Å, β = 90.11 (2)°, and V = 159.96 (2) Å^3 (space group $P2_1/m$) in good agreement with previous reports. For comparison, the XRD pattern of the sample obtained at 3 GPa is shown in Figure 5b. The XRD profile indicates that the sample prepared at 3 GPa is less crystalline than the one obtained at 4 GPa, and a small amount of an unidentified low-crystalline impurity phase is present (note peaks at 14.30 and 23.48 2θ in the inset in Figure 5b). In spite of the broadness and asymmetry of the peaks, the diffraction maxima of the 3 GPa sample's pattern could also be assigned to the β-V_2O_5 cell. Thus, experimental results are in good agreement with the transition pressure estimated from the computational study (3.3 GPa). There is also a good agreement with the $P-T$ phase diagram reported by Balog et al.,[16] where at 800 °C, the value used in our experiments, 3 GPa is enough for the phase transition to occur. Note that under our experimental conditions, at the highest limit of pressure (8 GPa), α-V_2O_5 still transforms into the β-V_2O_5 polymorph. Thus we could not find any evidence of the third V_2O_5 polymorph, as reported in previous works performed at similar pressures.[17,28] In fact, from the revisted phase diagram,[16] the pressure for the $\beta \rightarrow \delta$ transition at 800 °C, would be only slightly lower that 9 GPa.

The particle size and morphology of β-V_2O_5 was studied by SEM. Figure 6a shows a micrograph of commercial (α) V_2O_5 which consists of aggregates of thin platelets particles of hexagonal shape with a wide size distribution. In β-V_2O_5 (Figure 6b), although some large and massive particles are observed, the sample mainly consists of small needlelike particles. As shown in Figure 6c and d, the particle size is smaller as the pressure gets higher. The combined effect of

(29) Loa, I.; Grzecnik, A.; Schwarz, U.; Syassen, K.; Hanfland, M.; Kremer, R. K. *J. Alloys Compds.* **2001**, *317−318*, 103−108.

(30) Grzecnik, A. *Chem. Mater.* **1998**, *10*, 255−265.

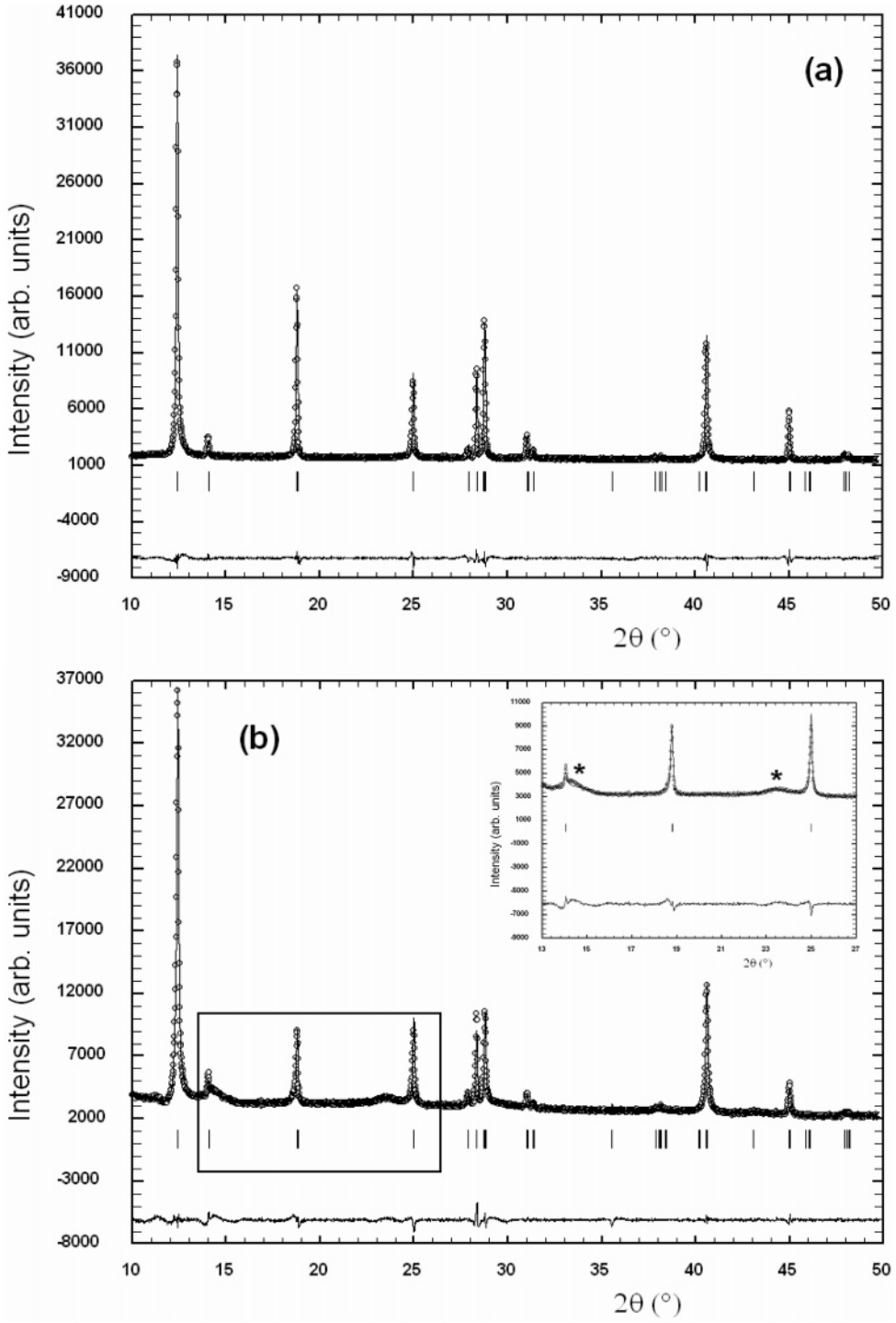

Figure 5. Profile refinement of XRD patterns corresponding to a β-V_2O_5 material prepared at (a) 4 and (b) 3 GPa. In the inset of panel b, two broad peaks of a low-crystalline unidentified impurity are indicated by asteriks. Observed (circles), calculated (solid line), and their difference. The Bragg peaks are indicated by vertical bars.

high pressure and heat treatment results in a decreasing particle size, meaning that no intermediate liquid phases are produced and that the phase transformation breaks the particles of the starting α-V_2O_5.

The structure of β-V_2O_5 is retained at ambient pressure, and after the long-term cycling of lithium cells, even though at ambient pressure it is metastable with respect to that of the α-form. The stability of β-V_2O_5 has been checked by DSC measurement (see Figure 7); this HP polymorph reverts to the ambient pressure one throughout an exothermic process with an associated energy of -186 J/g. The fact that the transformation starts at 220 °C is consistent with the observed stability of β-V_2O_5 as electrode in lithium batteries. The transformation process occurs in a wide range of temperature, being fully completed at 425 °C. During the DSC experiment on β-V_2O_5, increasing the temperature (at $p = 0$) has two effects: (i) it enables the material to transform more easily (kinetics), and (ii) it decreases the Gibbs free energy of the softer AP-phase (lower B) relative to that of the HP phase, thus increasing the thermodynamic driving force for the

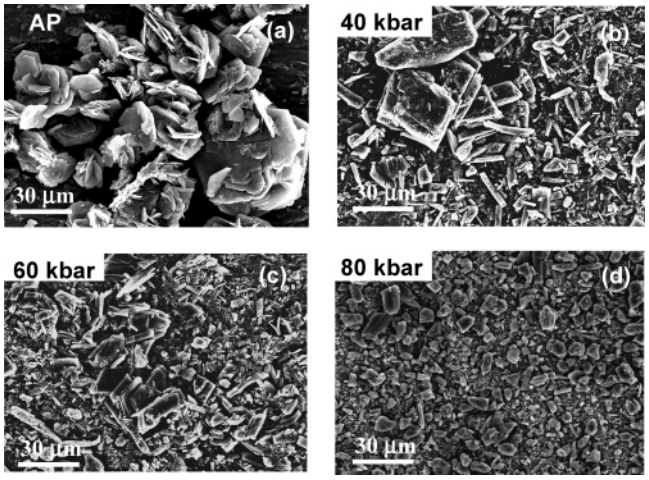

Figure 6. SEM micrographics of the (a) starting V_2O_5 and β-V_2O_5 prepared at (b) 4, (c) 6, and (d) 8 GPa.

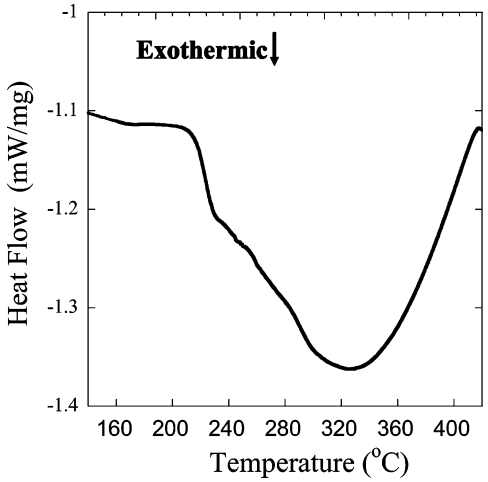

Figure 7. DSC curve of β-V_2O_5 heated in an O_2 atmosphere.

transformation. When the material finally undergoes the transformation at $p \approx 0$ and $T = 425$ °C

$$\Delta G_{p=0}(T = 698\ \text{K}) = G_{\text{AP}}(698\ \text{K}) - G_{\beta}(698\ \text{K}) = -186\ \text{J/g} \quad (2)$$

$$\Delta G_{p=0}(T = 698\ \text{K}) = G_{\text{AP}}(698\ \text{K}) - G_{\beta}(698\ \text{K}) = H_{\text{AP}} - TS_{\text{AP}} - H_{\beta} + \text{TS}_{\beta} = (H_{\text{AP}} - H_{\beta}) - (TS_{\text{AP}} - TS_{\beta}) \quad (3)$$

From the computational data of Table 3, $\Delta H_{p=0} = E_{\text{AP}} - E_{\beta} = -92$ J/g. The enthalpy at $p = 0$ is the bare energy, which gives

$$\Delta G_{p=0}(T = 698\ \text{K}) = (E_{\text{AP}} - E_{\beta}) - (TS_{\text{AP}} - TS_{\beta}) = -92\ \text{J/g} - T(S_{\text{AP}} - S_{\beta}) \quad (4)$$

This is to say, the bare energy difference at $T = 0$ and the measured exothermic energy at finite T *should* not agree exactly, as they differ from each other in the TΔS term. Since the AP phase is softer, $T(S_{\text{AP}} - S_{\beta}) > 0$ and the $\Delta G_{p=0} < -92$ J/mol, in good agreement with experiments.

Electronic Structure and Properties of α-V_2O_5 and β-V_2O_5. *Computational.* Figure 8 shows the calculated total density of states (DOS) of α-V_2O_5 (a) and β-V_2O_5 (b), together with the partial DOS of vanadium (green line) and oxygen (red line). An isolated vanadium V^{5+} ion contains

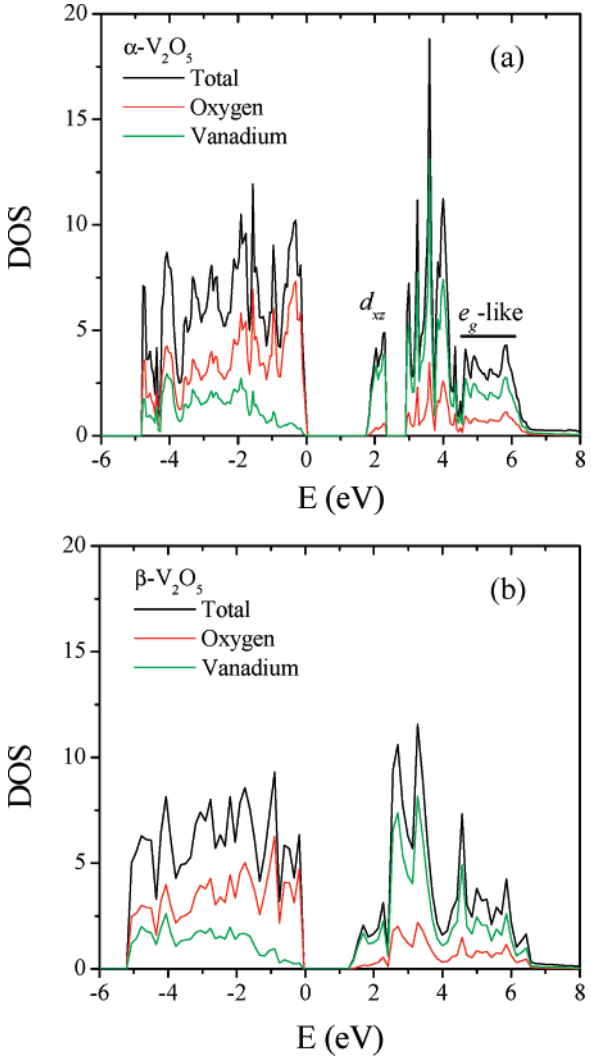

Figure 8. Calculated density of states (DOS) in states/fu of (a) α-V_2O_5 and (b) β-V_2O_5 compounds. The gray lines denote the total DOS; the partial DOS of vanadium and oxygen are represented in green and red lines, respectively. The Fermi level has been arbitrarily chosen as the origin of the energy.

no occupied d-orbitals. This means that any d-character in the DOS below the Fermi level is a direct result of oxygen−vanadium interactions. The σ overlap between V-3d and O-2p orbitals results in the bonding σ-band, which appears below the Fermi level (predominantly oxygen-2p in character), and the σ*-band above the Fermi level (mostly consisting of vanadium-3d states). The significant mixing of O-2p states and V-3d states in both the σ- and σ*-bands supplies direct evidence for the strong covalent interaction of the V−O bonds. The vanadium $3d_{xy}$-, d_{xz}-, and d_{yz}-orbitals are involved in π-interactions with the filled oxygen p-orbitals of appropriate symmetry. The bonding t_{2g}-bands appear in the valence band dominated by oxygen-2p states and the antibonding t_{2g} states right above the Fermi level. In a perfectly cubic octahedral environment, the antibonding t_{2g} bands are degenerate. In α-V_2O_5, however, the square pyramidal coordination of the V^{5+} ions causes the splitting of the t_{2g}-like band into two sets of bands: the upper $3d_{xy}$/d_{yz} one and the $3d_{xz}$ bottom one centered at 2 eV (note that in the coordinate system used in the calculations the vanadyl bond is along the *b*-axis). In the β-V_2O_5 DOS, such a

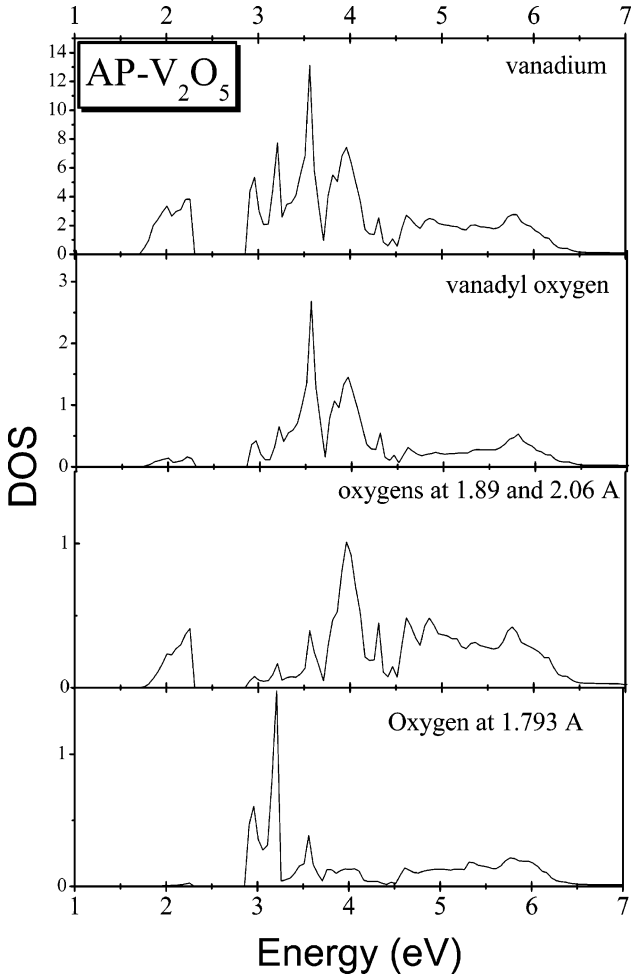

Figure 9. Calculated partial DOS of vanadium and surrounding oxygen ions (see Figure 2) in α-V_2O_5.

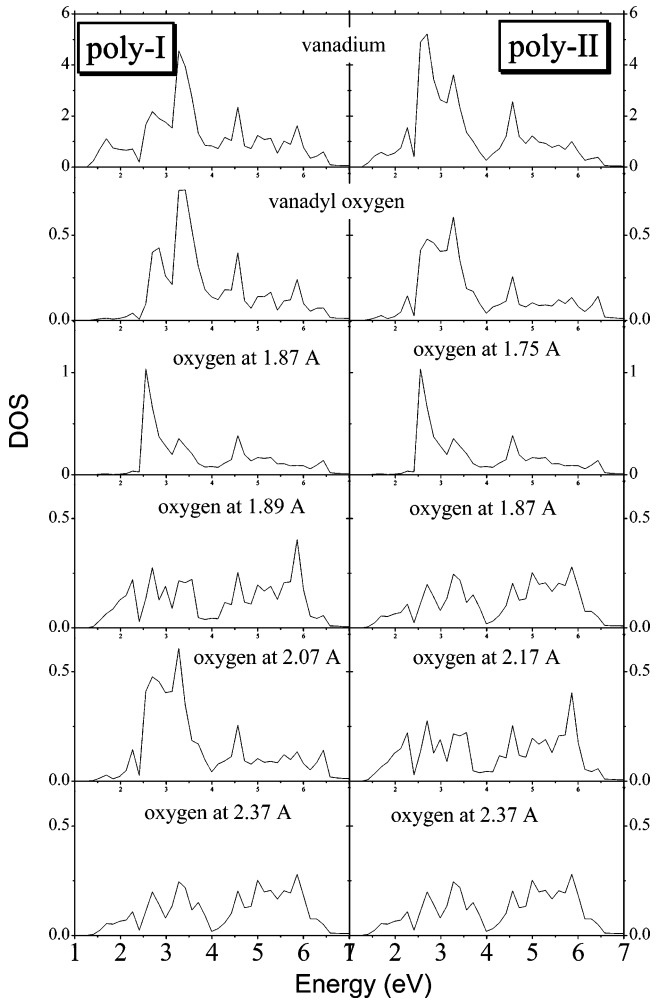

Figure 10. Calculated partial DOS of vanadium and oxygen ions in β-V_2O_5. Left and right panels correspond to the vanadium polyhedra denoted as poly-I and poly-II, which are shown in Figure 2c and b, respectively.

pronounced splitting of the conduction band is not observed, although the high distortion of the V octahedra (see Figure 2) still breaks the degeneration of the t_{2g}-like band. The calculated band gap for α-V_2O_5 of 1.74 eV is in excellent agreement with previous DFT studies (LDA, 1.74 eV;[31] GGA, 1.75 eV)[32] but is below the experimentally measured optical gap (2.2 eV).[33] A recent work within the DFT+U framework provides a calculated band gap of 2.1 eV,[34] confirming the fact that a Hubbard-like correction term (U) substantially improves the accuracy of the calculated band gap. As shown in Figure 8b, the calculated gap in β-V_2O_5 is 1.24 eV, this is, 0.5 eV narrower than in the ambient-pressure polymorph. Notice that the different color of the samples, (black-reddish for the HP material (β-V_2O_5) and orange for AP material), is in good agreement with the predicted decrease of the optical gap.

Figure 9 shows the partial V-3d DOS (upper panel) together with the partial DOS of the different oxygen atoms in their local environment in α-V_2O_5 (see Figure 2). It can be seen that the split-off conduction band (centered at 2 eV) mostly originates from the π-overlapping between V-3d-orbitals and the p-orbitals of the basal oxygens, at 1.89 and 2.06 Å. The remaining t_{2g}-like band, appearing between 3 and 4.5 eV, is caused by the shorter V−O bonds, this is, the vanadyl bond and the bond with the basal oxygen at 1.79 Å. The larger the π-type overlap, the larger the bonding-antibonding splitting is. Thus, bands with dominant contributions from the larger V−O bond length experience a smaller bonding−antibonding splitting and hence their antibonding bands remain at lower energies, relative to the valence-band maximum. In contrast, the strong vanadyl bond causes its corresponding states to separate from the lower-energy unoccupied states, opening a gap in the conduction band.

Figure 10 shows the partial V-3d DOS (upper panel) together with the partial DOS of its bonded oxygens, in β-V_2O_5, where two different vanadium polyhedra are present (see Figure 2). As discussed above, both vanadium ions present a distorted octahedral coordination. The split-off conduction band, characteristics of V^{5+} in a square pyramid environment, is not observed; this is because the reduction in the $Vd-O_{vanadyl}p$ π-overlap causes the downshift of the vanadyl derived states and the disappearance of the split-off band. Notice that in poly-I, the calculated short V−O bond length (1.59 Å) is only slightly shorter than the one calculated in α-V_2O_5 (1.60 Å). Hence, the decrease in the effective

(31) Eyert, V.; Höck, K. H. *Phys. Rev. B* **1998**, *57* (20), 12727.
(32) Willinger, M.; Pinna, N.; Su, D. S.; Sclögl, R. *Phys. Rev. B* **2004**, *69*, 155114.
(33) Kenny, N.; Kennewurf, C. R.; Whitmore, D. H. *J. Phys. Chem. Solids* **1966**, *27*, 1237.
(34) Wang, L.; Maxisch, T.; Ceder, G. *Phys. Rev. B* **2006**, *73*, 195107-1−195107-6.

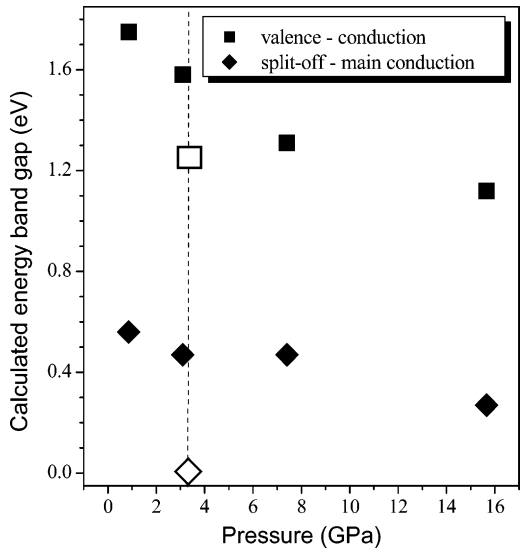

Figure 11. Calculated pressure dependence of the energy gap in α-V_2O_5 (space group *Pmnm*) between the valence and conduction band (square symbol) and between the slipt-off and the main conduction band (diamond symbol). The dashed line indicates the pressure of the transformation to the *β*-V_2O_5 (3.3 GPa); the white symbols correspond to the calculated energy gap in the *β*-V_2O_5.

overlapping of the Vd−$O_{vanadyl}$p π in *β*-V_2O_5, compared to that in α-V_2O_5, is rooted not only in the vanadyl bond length but also in the presence of a sixth V−O bond. The split-off conduction band (centered at 2 eV) in a V_2O_5 widens in *β*-V_2O_5 than that in α-V_2O_5, leading to a narrow energy gap between the valence and the conduction band. As expected, the states derived from the long V−O bond have a major contribution at the bottom of the conduction band. In summary, the 6-fold coordination of vanadium ions in *β*-V_2O_5 has two effects: (i) merging of the split-off conduction band characteristic of the square pyramidal coordination and (ii) narrowing of the energy gap between the valence and conduction bands.

The changes in the electronic structure as a function of the pressure can be followed in the AP-polymorph (*Pmnm* symmetry), parallel to the structural parameters and bond length shown Figure 4. The results plotted in Figure 11 confirm that pressure induces a narrowing of the energy band gap between the valence and conduction band. Although an energy gap still exists between the split-off and the main part of the conduction band, the general trend is to close this gap as pressure increases. These results are consistent with those of Eyert et al.,[31] who reported a calculated band structure of hypothetical V_2O_5 with vanadium ions in a perfect cubic octahedral symmetry. They found that imposing a cubic symmetry to the V_2O_5 structure leads to a semimetal compound, where the valence and conduction bands share a common energy range of about 0.3 eV, and with no splitting in the conduction band (i.e., both gaps represented in Figure 11 reach a zero value). Note that imposing such a cubic octahedral symmetry causes the vandayl bond to elongate (single bond), which means that the results of Eyert et al. could be taken as the case of a V_2O_5 structure under extreme pressure. Hence, *β*-V_2O_5 might be considered to be an intermediate structure between the AP polymorph (vanadium ions in square pyramid) and the hypothetical "high-symmetry" V_2O_5 (vanadium ions in perfect cubic symmetry).

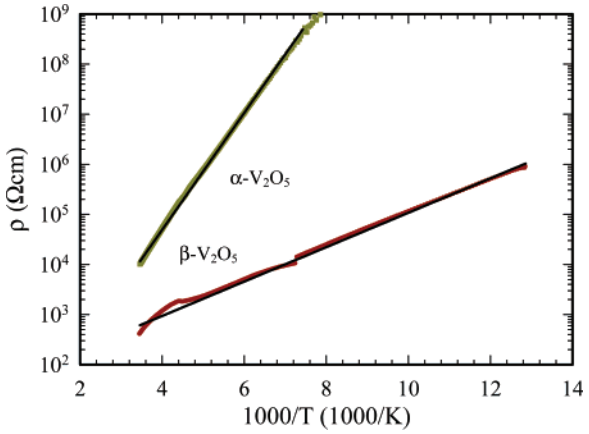

Figure 12. Resistivity of α-V_2O_5 and *β*-V_2O_5 polymorphs versus inverse temperature. Black lines are fit to $\rho = \rho_0 \exp(E_A/kT)$.

Even more, the *δ*-V_2O_5 polymorph, despite having a 3D structure, is still far from this high-symmetry octahedral environment of V^{5+}; indeed, the VO_6 octahedra are distorted, and the vanadium atom is displaced from the center toward one corner of the octohedron; thus a V−O distance as short as 1.628 Å exists in this phase as in the other two polymorphs. Therefore, the expected electrical properties of this *δ*-V_2O_5 phase should be similar to that of the *β*-polymorph. It is obvious the interest of performing both ab initio calculations of its electronic structure and experimental measurements of the electrical properties.

Experimental. DC conductivity was measured on both the α- and *β*-polymorphs of V_2O_5 from room temperature down to $T = 77$ K. As shown in Figure 12, the room-temperature resistivity decreases by more than 1 order of magnitude, from 10000 Ω cm in α-V_2O_5 to 400 Ω cm in *β*-V_2O_5. The α-V_2O_5 resistivity is 10 times smaller than those reported for single crystals and is probably the result of impurities in commercial V_2O_5 powder. In the above temperature window, the resistivities of both compounds show activated behavior with activation energies, E_A, of 0.232 and 0.068 eV for the α- and *β*-polymorphs, respectively. This suggests that in the *β*-polymorph, consisting of VO_6 octahedra and not VO_5 square pyramids, electrical conductivity is strongly enhanced. Note also that the measured activation energy for α-V_2O_5 gives an energy gap, $\Delta_T = 2E_A = 0.46$ eV, much smaller than optical band gap, $\Delta_O = 2.2$ eV.[33] This discrepancy between the optical and the transport measurements has been assigned to small polarons.[35] A similar difference is found in *β*=V_2O_5 ($\Delta_T = 2E_A = 0.14$ eV and calculated band gap $\Delta_O = 1.24$ eV) suggesting that a polaron conduction mechanism also operates in this material.

Concluding Remarks

We have investigated the pressure-induced transformation of V_2O_5 into its high-pressure polymorph *β*-V_2O_5 combining first principles and experimental methods. DFT predicts that α-V_2O_5 transforms to *β*-V_2O_5 at 3.3 GPa with a 11.6% volume reduction. Experiments corroborate that V_2O_5 ($d = 3.36$ g/cm^3) transforms at 800 °C and a pressure of 4 GPa into a well-crystallized *β*-V_2O_5, which possesses a 11.8%

(35) Loffe, V. A.; Petrina, J. B. *Phys. Stat. Sol.* **1970**, *40*, 389.

denser structure ($d = 3.76$ g/cm^3). β-V_2O_5 can even be prepared at 3 GPa, though with a substantial degree of amorphization. These results support a much smaller pressure for the $\alpha \rightarrow \beta$ transition than previously reported (6 GPa), which is economically beneficial in the view of possible electrochemical applications for β-V_2O_5.

The calculated DOS shows a narrowing of about 0.5 V in the band gap for the β-polymorph in comparison with the α one, mostly because of the octahedral coordination of vanadium ions in the former. The measured resistivites at room temperature (10 000 Ω cm in α-polymorph and 400 Ω cm in β-polymorph, respectively) reveal that the HP polymorph is indeed a better electronic conductor than the AP one. High-power lithium batteries depend on fast lithium insertion reaction, requiring good ionic/electronic motion of lithium ions/electrons across the electrode material. Thus, the enhanced electronic conductivity of β-V_2O_5 with respect to that of the ambient pressure form is a major advantage in terms of electrochemical applications.

Although the V_2O_5 $\alpha \rightarrow \beta$ transformation proceeds through a complex two-step mechanism,[17] computational data suggest that a crucial factor is the high compressibility of α-V_2O_5 along its *b*-axis (interlayer space). The long V−O distance in the structure is predicted to decrease significantly with pressure, thus increasing the vanadium coordination from five to six and leading to the stabilization of the β-polymorph. The change of the coordination environment around vanadium ions from square pyramids in α-V_2O_5 to octahedral in β-V_2O_5 is also the cause of the changes in the electronic structure. It is expected that a similar transformation would occur in other layered structures based on V^{5+} in square-pyramid coordination under moderate pressure. Given the potential interest of V^{5+} compounds as electrode for lithium batteries, this opens a new path for synthesis of interesting novel electrochemically active materials with improved electronic conductivity.

Given that we used both first principles computations and experiments to search for the high-pressure polymorph of V_2O_5, it is interesting to consider whether this structure could have been found by computations alone. Searching for ground state structures in a material requires both a good energy model and an effective strategy to search through the infinite number of possible atomic arrangements. In metals, the predictive accuracy of density functional theory in the GGA approximation is very high[36] so that the identification of good candidate structures to calculate has become the limiting factor. A recent method which suggests candidate structures by data-mining correlations between other structures in the system and a large database of known compounds[37,38] has not been evaluated on oxides yet. The structure of β-V_2O_5, although related to that of MoO_3, is rather uncommon; to the best of our knowledge, the same structural skeleton is present solely in $TMAV_8O_{20}$ (TMA = tetramethylammonium), where the large TMA cations are located between the V_4O_{10} double layers.[9] Therefore, it is doubtful that this structure could have been truly suggested on the basis of data-mining techniques. On the other hand, genetic algorithm-based searching techniques,[39] which merge and mutate parts of low-energy structures to find even lower-energy structures, may be applicable to this system; although in transition metal oxides, the accuracy of GGA in obtaining the correct ground state may be less than that for metals.[40] This leaves experiments and computations still mutually benefiting from each other in the search for high-pressure polymorphs with improved properties. The possibility of estimating the order of the transition pressure between two polymorphs is a valuable information to guide the experimental work. Presented with a structural hypothesis from experimental observations, computations can be used to verify the plausibility of this hypothesis. On the other hand, experiments are limited to structures that can actually be formed, making it impossible to follow the structural evolution of a polymorphic form at pressures beyond its range of stability. This work illustrates the utility of computational investigations to anticipate changes of the properties of "real materials" that might occur in a wide range of pressures.

Acknowledgment. This work was supported by Universidad Complutense de Madrid (PR1/07-14911), the Spanish MEC (MAT2004-03070, and "Ramon y Cajal" program), and CAM (S-0505/PPQ-0093). Calculations were performed at the CIEMAT Supercomputing Centre. Authors are grateful to M. J. Torralvo and B. Levenfeld for the DSC data and to P. Rozier for his valuable comments.

CM071360P

(36) Curtarolo, S.; Morgan, D.; Ceder, G. *Comput Coupling Phase Diagrams Thermochem.* **2005**, *29*, 163−211.
(37) Fischer, C. C.; Tibbetts, K. J.; Morgan, D.; Ceder, G. *Nat. Mater.* **2006**, *5* (8), 641.
(38) Curtarolo, S.; Morgan, D.; Persson, K.; Rodgers, J.; Ceder, G. *Phys. Rev. Lett.* **2003**, *91* (13), 135503-1−135503-4.
(39) Oganov, A. R.; Glass, C. W. *J. Chem. Phys.* **2006**, *124*, 244704.
(40) Zhou, F.; Marianetti, C. A.; Cococcioni, M.; Morgan, D.; Ceder, G. *Phys. Rev. B* **2004**, *69*, 201101(R).